Celest Mech Dyn Astr (2008) 101:309–320
DOI 10.1007/s10569-008-9147-4

ORIGINAL ARTICLE

Vertical bifurcation families from the long and short period families around the equilateral equilibrium points

X. Y. Hou · L. Liu

Received: 24 November 2007 / Revised: 28 April 2008 / Accepted: 14 May 2008 /
Published online: 24 June 2008

Abstract In this paper, following the increase of the mass ratio μ, the vertical stability curves of the long and the short period families were studied, and the vertical bifurcation families from these two families were computed. It is found that these vertical bifurcation families connect the long and short period families with the spatial periodic family emanating from the equilateral equilibrium points. The evolution details of these vertical bifurcation families were carefully studied and they are found to be similar to the planar bifurcation families connecting the long period family with the short period family in the planar case.

Keywords Restricted three-body problem · Equilateral equilibrium point · Periodic orbit · Bifurcation

1 Introduction

The equilateral libration points of the circular restricted three-body problem are equilibrium points of elliptic type in the planar case for $\mu < \mu_1 = 0.0385\ldots$. There are two fundamental frequencies ω_s and ω_l, with $\omega_s > \omega_l$. For the out-of-plane motion, it is always stable, with a linearized fundamental frequency $\omega_z = 1$. According to Lyapunov's theorem, there are three periodic families emanating from the equilibrium points. For the planar case, there are the long period family and the short period family corresponding to the frequencies ω_l and ω_s respectively (Szebehely 1967). For the vertical case, there is the three dimensional periodic family corresponding to the frequency ω_z (Zagouras 1985). In the following, for brevity, we call the three dimensional periodic family as 3D periodic family.

X. Y. Hou · L. Liu (✉)
Astronomy Department, Nanjing University, Nanjing 210093, China
e-mail: lliu@nju.edu.cn

X. Y. Hou
e-mail: xiyun.hou@gmail.com

X. Y. Hou · L. Liu
Institute of Space Environment and Astronautics, Nanjing University, Nanjing 210093, China

There are planar bifurcation orbits and vertical bifurcation orbits in the long and short period families (Hénon 1973). For planar bifurcation orbits, there are periodic families connecting them. These families are often called bridges and have been widely studied (Deprit and Henrard 1968; Henrard 2002; Bruno and Varin 2007). However, seldom work has been done about the vertical bifurcation orbits (Perdios and Zagouras 1991; Bruno and Varin 2006). We wonder whether these vertical bifurcation orbits are connected with some bifurcation orbits in a special periodic family, as what happens in the planar case. Following this idea, we continued the vertical bifurcation families bifurcating from the long and short period families to their natural ends. We found this special periodic family does exist and it is just the 3D periodic family.

In this paper, following the increase of μ, the vertical stability curves of the long and short period families were firstly studied. Then the stability curves of the 3D periodic family with increasing μ were also studied. At last the vertical bifurcation families connecting the long and short period families with the 3D families were studied.

2 Methodology

The usual synodic coordinate for the circular restricted three-body problem is shown in the left figure of Fig. 1. For clarity, we didn't plot the z axis which is perpendicular to the $x-y$ plane. The coordinate we choose to analyze the periodic orbits, however, is not the usual synodic one. It has its origin at the equilateral equilibrium points and rotates the $x-y$ plane with a fixed angle α, where α is a constant of μ. We didn't plot the z axis which is perpendicular to the $\xi-\eta$ plane either. About the details of this coordinate, the reader can refer to the book of Szebehely (1967).

In fact, we give initial conditions of periodic orbit in the $\xi\eta z$ frame, transfer them to the synodic one and integrate the orbits. After period T, we transfer the states of orbits in the synodic coordinate back to the $\xi\eta z$ frame to check the periodic conditions. The algorithm used to continue periodic families is the usual predictor-corrector one. The reader can turn to the references for more details (Deprit and Henrard 1967). In this paper, all the periodic families are computed this way.

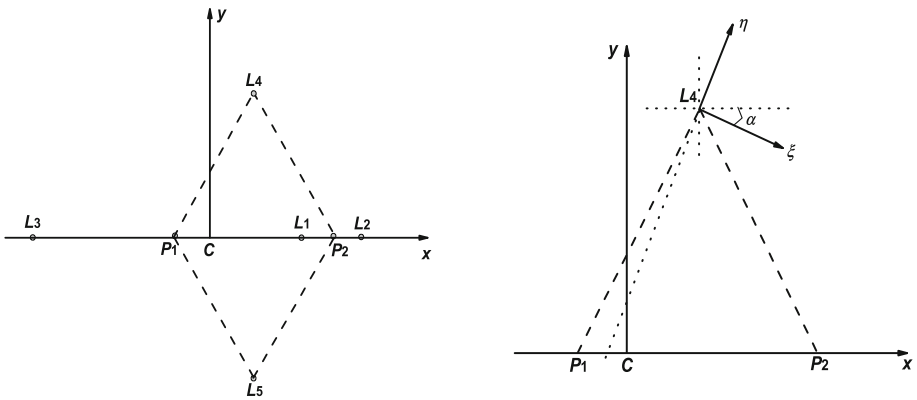

Fig. 1 The synodic coordinate and coordinate chosen in our work

The integrator we used is the traditional RKF78 integrator. The accuracy of the refinement is guaranteed to be around 10^{-8}.

3 Results

3.1 Vertical stability curves of the long and short period families

For the planar case, there are critical mass ratios when ω_s and ω_l are in commensurability. These mass ratios are (Szebehely 1967)

$$\mu_k = [1 - (k^4 + 38k^2/27 + 1)^{1/2}/(k^2 + 1)]/2 \tag{1}$$

where $k = q/p, q, p$ are integers. Similarly, we denote the mass ratios when ω_l and ω_z are in commensurability as μ'_k, it satisfies

$$\mu'_k = \frac{1}{2}\left\{1 - \sqrt{1 - 4[1 - (1 - 2/k^2)^2]/27}\right\} \tag{2}$$

where $k = q/p$. For mass ratios where ω_s and ω_z are in commensurability, the same formula exists, but with $1 < k = q/p < \sqrt{2}$. It's easy to check the following relations.

$$\mu'_{k+1} < \mu_k < \mu'_k \tag{3}$$

Although μ'_k are not critical values concerning the evolution of the long period family, we introduce them for better understanding the evolution details of the vertical stability curves of the long and short period families.

First, we study the vertical stability curve of the long period family. When $\mu = \mu'_{k+1}$, the stability index reduces from 2 with the increasing amplitude of long period orbits and then increases again. When the long period family terminates onto a planar critical short period orbit, the vertical stability index does not equal 2. So the termination of the long period family is not a vertical critical short period orbit. Shown in Fig. 2 is the stability curve for $\mu = \mu'_6$. The ordinate "$TraceV$" equals $(a_{33} + a_{66} - 2)$, where $M = (a_{ij})_{6\times 6}$ is the monodromy matrix of the periodic orbit.

Following the increase of μ from μ'_{k+1} to μ'_k, the origin of the stability curve (denoted as L_4 in Fig. 2) will first reduces to a little smaller than -2 and than increases again to 2. The turning point is $\mu = \mu'_{(2k+1)/2}$. Between μ'_{k+1} and μ'_k exists the critical mass ratio μ_k. The structure of the long period family changes (Deprit and Henrard 1968), so changes with it the vertical stability curve. In Fig. 3, from left to right and from top down, local magnifications of the vertical stability curve around the origin for different mass ratios μ'_6, $\mu'_6 - 1 \times 10^{-4}$, $\mu'_{11/2}$, $\mu_5 - 1 \times 10^{-4}$, $\mu_5 + 1 \times 10^{-4}$ and μ'_5 are given. The abrupt changes between the fourth and the fifth figures are due to the structure changes of the long period family at μ_5.

The evolution scenario is valid only for $k \geq 5$. When $k < 5$, there is another special critical value between μ'_{k+1} and μ'_k besides the critical value μ_k (Henrard 1970; Hou and Liu 2008a). Take $k = 3$ for an example. Between μ'_4 and μ'_3 exists a special critical value μ^* (Henrard 1970), the long period family changes its structure at this critical value, so does the vertical stability curve. In Fig. 4, from left to right and from top down, local magnifications of the vertical stability curve around the origin for different mass ratios μ'_4, $\mu'_4 < 0.0122 < \mu^*$, $\mu^* < 0.0124 < \mu_3$, $\mu_3 - 1 \times 10^{-4}$, $\mu_3 + 1 \times 10^{-4}$ and μ'_3 are given. The abrupt changes between the second and the third figures are due to the structure changes of the long period family at μ^*.

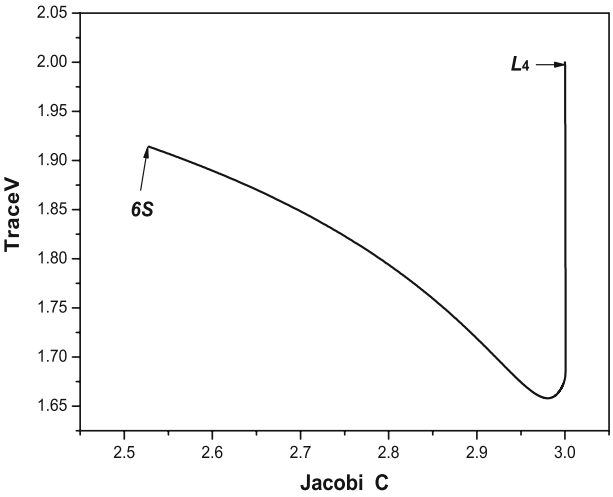

Fig. 2 The vertical stability curve of the long period family for $\mu = \mu'_6$

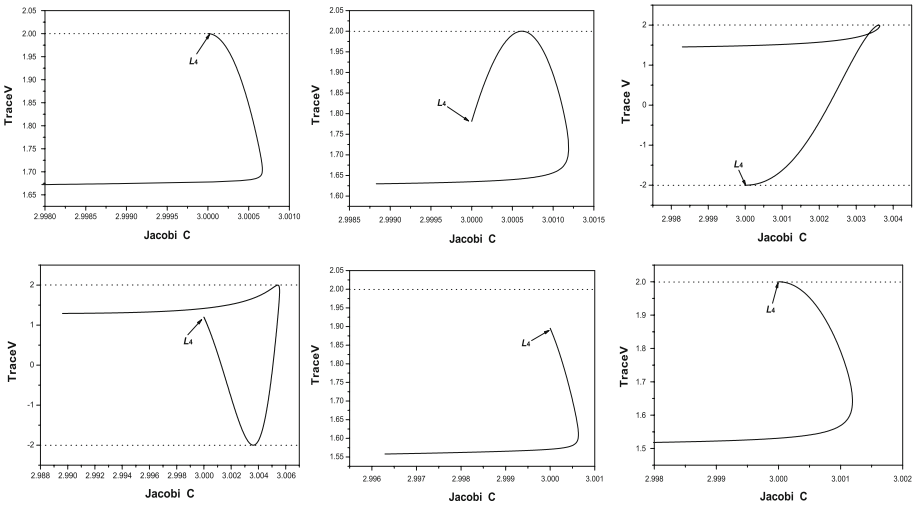

Fig. 3 The vertical stability curves of the long period families for different mass ratios between μ'_6 and μ'_5

To save space, we will not explain the details of the abrupt changes of the long period family at these critical mass ratios. Readers can refer to references for more details (Deprit and Henrard 1968; Henrard 1970; Hou and Liu 2008a). We just have to know that the following general evolution tendency holds true: with μ increasing from μ'_{k+1} to $\mu'_{(2k+1)/2}$, the origin of the vertical stability curve reduces; with μ increasing from $\mu'_{(2k+1)/2}$ to μ'_k, the origin of the vertical stability curve increases. More specifically, when $\mu < \mu'_{q/p} < \mu'_{(2k+1)/2}$, the origin of the vertical stability curve is larger than $2\cos(q \cdot 2\pi/p)$; when $\mu > \mu'_{q/p} < \mu'_{(2k+1)/2}$, the origin is smaller than $2\cos(q \cdot 2\pi/p)$; when $\mu < \mu'_{q/p} > \mu'_{(2k+1)/2}$, the origin of the vertical stability curve is smaller than $2\cos(q \cdot 2\pi/p)$; when $\mu > \mu'_{q/p} > \mu'_{(2k+1)/2}$, the origin of the vertical stability curve is larger than $2\cos(q \cdot 2\pi/p)$.

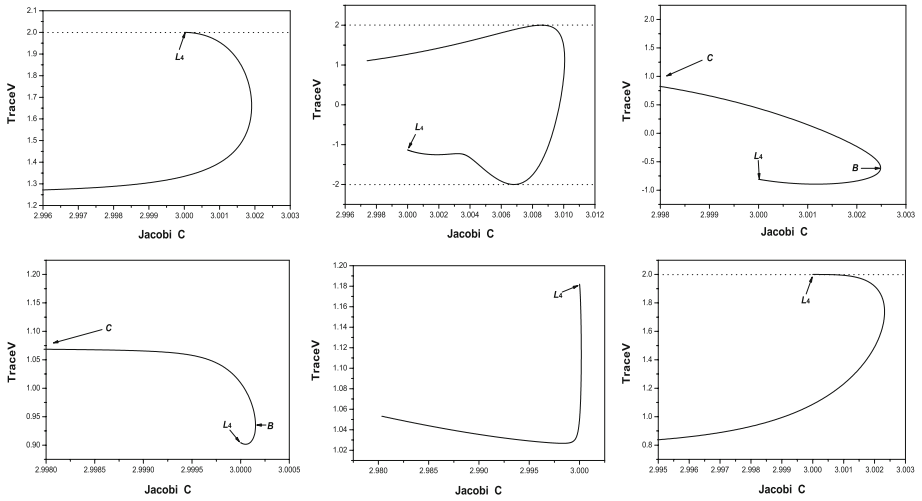

Fig. 4 The vertical stability curves of the long period families for different mass ratios μ_4' and μ_3'

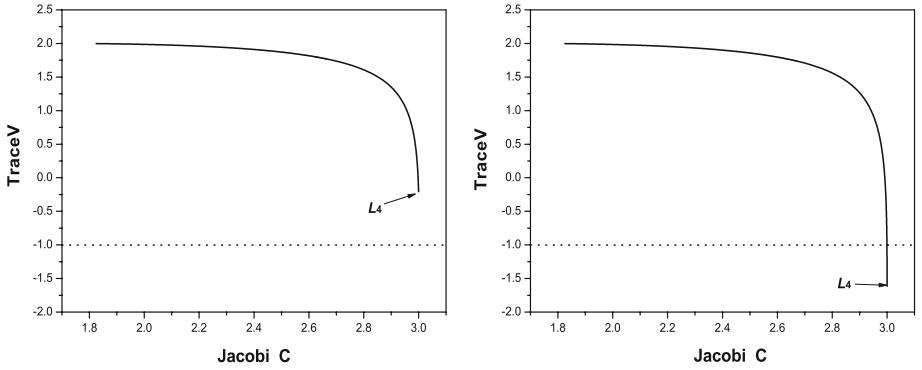

Fig. 5 The vertical stability curve of the short period family for mass ratios $\mu_{3.8/3}$ and $\mu_{4.2/3}$

The vertical stability curve of the short period family is much simpler. Following the increase of μ, the origin of the stability curve reduces. More specifically, when $\mu < \mu'_{q/p}$ (where $1 < q/p < \sqrt{2}$), the origin of the vertical stability curve is larger than $2\cos(q \cdot 2\pi/p)$; when $\mu > \mu'_{q/p}$, the origin of the vertical stability curve is smaller than $2\cos(q \cdot 2\pi/p)$. Take $q/p = 4/3$ as an example, Fig. 5 are the vertical stability curves for mass ratios $\mu'_{3.8/3} < \mu'_{4/3}$ and $\mu'_{4.2/3} > \mu'_{4/3}$. Because $q/p < \sqrt{2}$, the origin of the vertical stability curve of the short period family cannot be smaller than $2\cos(2\pi/\sqrt{2})$. So there is no vertical 2-bifurcation short period orbit. The maximal possible value for q/p is $4/3$.

3.2 The 3D periodic family

Zagouras has given formulas for the 3D periodic family up to fourth order (Zagouras 1985). These formulas can be used as initial seed for the predictor-corrector algorithm mentioned

above. The eigenvalues of the monodromy matrix M can be solved from the following equation (Bray and Goudas 1967).

$$(\lambda - 1)^2(\lambda^2 + p_1\lambda + 1)(\lambda^2 + p_2\lambda + 1) = 0 \tag{4}$$

where

$$p_1 = \frac{1}{2}(\alpha + \sqrt{D}),\ p_2 = \frac{1}{2}(\alpha - \sqrt{D}),\ D = \alpha^2 - 4(\beta - 2)$$
$$\alpha = 2 - Tr(M),\ \beta = \frac{1}{2}[\alpha^2 + 2 - Tr(M^2)]$$

Obviously, there are two stability curves, we denote them as curve p_1 and curve p_2. With the increase of μ, the origin of the curve p_1 (denoted as L_4 in the figures) will raise first and then reduces. The turning point is $\mu = \mu'_2$. More specifically, when $\mu < \mu'_{q/p} < \mu'_2$, the origin of the curve p_1 is smaller than $-2\cos(p \cdot 2\pi/q)$; when $\mu > \mu'_{q/p} < \mu'_2$, the origin of the curve p_1 is larger than $-2\cos(p \cdot 2\pi/q)$. When $\mu < \mu'_{q/p} > \mu'_2$, the origin of the stability curve p_1 is larger than $-2\cos(p \cdot 2\pi/q)$; when $\mu > \mu'_{q/p} > \mu'_2$, the origin of the stability curve p_1 is smaller than $-2\cos(p \cdot 2\pi/q)$. For the curve p_2, the origin always increases with increasing μ. More specifically, when $\mu < \mu'_{q/p}$, the origin is smaller than $-2\cos(p \cdot 2\pi/q)$; when $\mu > \mu'_{q/p}$, the origin is larger than $-2\cos(p \cdot 2\pi/q)$. When μ increases to $\mu'_{\sqrt{2}} = \mu_1$, the origins of the curves p_1 and p_2 coincide, with a stability index $-2\cos(2\pi/\sqrt{2})$ (Denoted as B in the last figure of Fig. 6). Shown in Fig. 6 are the stability curves for mass ratios μ'_4, μ'_2 and $\mu_{\sqrt{2}}$.

Numerical computations show that the vertical long period bifurcation orbits are connected with the bifurcation orbits in the stability curve p_1 and the vertical short period bifurcation orbits are connected with bifurcation orbits in the stability curve p_2.

3.3 Vertical bifurcation families

In the following, we take $\mu \in (\mu'_6, \mu'_5)$ as an example to show how the vertical bifurcation families evolve. We use P to denote members of the 3D periodic family. Shown in the left figure of Fig. 7 is the local magnification of the vertical stability curve of the long period family for the mass ratio $\mu'_{11/2} + 6 \times 10^{-4}$. "left" and "right" in the figure indicate two different long period orbits with vertical stability index 2. The two vertical long period bifurcation orbits are connected with a 6-bifurcation orbit in the 3D family with stability index $-2\cos(2\pi/6)$ in the curve p_1. The right picture gives out the T–C curves for the vertical families $B(L_{left}, 6P)$ and $B(L_{right}, 6P)$. We call these families as bridges as we did in the planar case (Deprit and Henrard 1968; Bruno and Varin 2007). Since the two long period orbits are too close to each other, we can't separate them in the figures. We just use "left" and "right" to indicate them. The curve denoted as "3D family" is the T–C curve of the 3D periodic family. The period of the 3D periodic orbits is multiplied 6 times in order to show it in the same figure as the families $B(L_{left}, 6P)$ and $B(L_{right}, 6P)$. Shown in Fig. 8 are the stability curves p_1 and p_2 for the two families, with the smooth one corresponding to the family $B(L_{right}, 6P)$. The unsmoothness of the stability curves is due to the following fact. In continuation of periodic families, we may encounter unstable members with eigenvalues of the $\lambda = \alpha + \beta i$, $|\lambda| > 1$ type. So p_1 or p_2 may be complex. That means D may be smaller than zero during the numerical continuation. In order to avoid this uncertainness, we take $|D|$ instead of D in Eq. 4, and this choice leads to the unsmoothness. Nevertheless, the validity

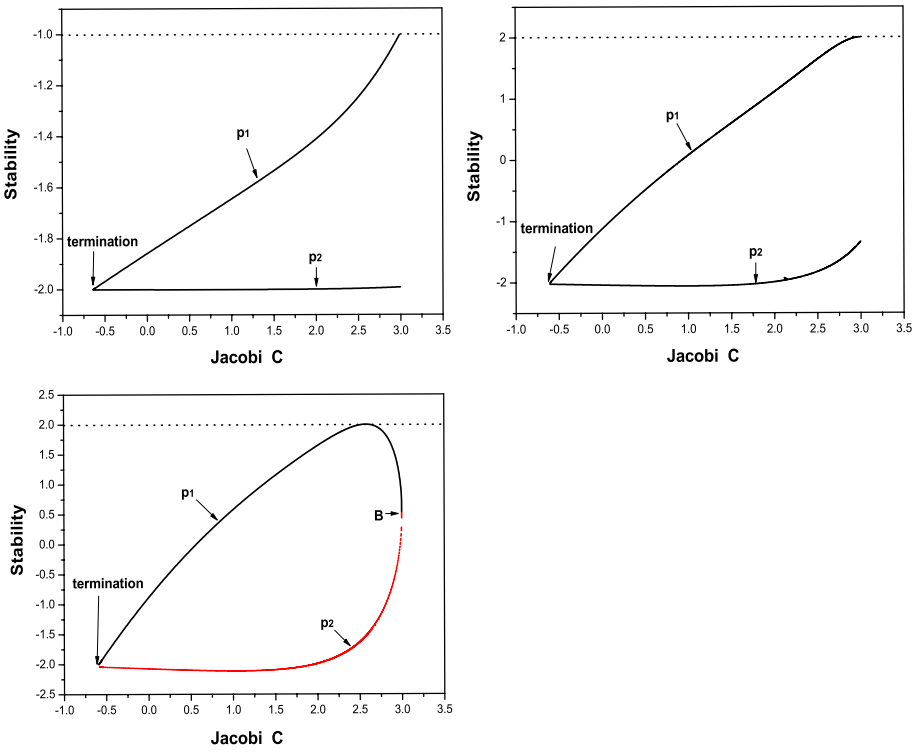

Fig. 6 Stability curves of the 3D family for mass ratios μ'_6, μ'_2 and $\mu'_{\sqrt{2}}$

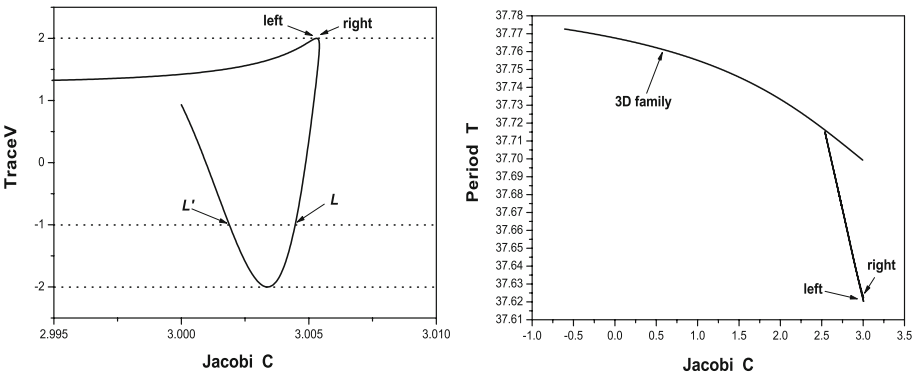

Fig. 7 The vertical stability curve for the mass ratio $\mu_{11/2} + 6 \times 10^{-4}$ and the T–C curves for the two vertical bifurcation families $B(L_{left}, 6P)$ and $B(L_{right}, 6P)$

of the continuation process can be guaranteed by the continuity of the T–C curves. Table 1 gives out initial conditions for the two bifurcation long periodic orbit. From left to right are values for x, y, $\dot{x}$, $\dot{y}$, T, C. Table 2 gives out initial conditions of one member of each family. In each row, from left to right are values for x, y, z, $\dot{x}$, $\dot{y}$, $\dot{z}$, T, C.

There are two 2-bifurcation long period orbits (with stability index -2) in the left figure of Fig. 7. They are also very close to each other. We cannot tell them in the figure. They

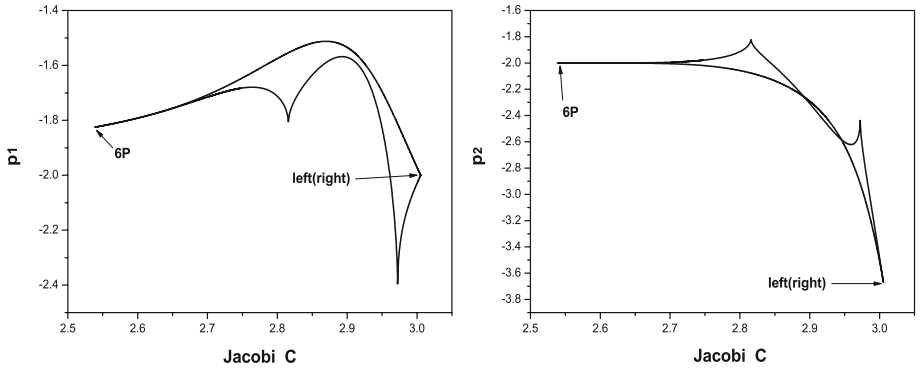

Fig. 8 The stability curves p_1 or p_2 for the two brides $B(L_{left}, 6P)$ and $B(L_{right}, 6P)$

Table 1 Initial conditions for the bifurcation long periodic orbit $left$ and $right$ in Fig. 7

Orbits	x	y	$\dot{x}$	$\dot{y}$	T	C
Left	0.55735842	0.97524293	0.17233433	−0.094181765	37.62225141	3.00530435
Right	0.55732988	0.97519323	0.17225074	−0.094122691	37.62028766	3.00530578

Table 2 Initial conditions for one member of families $B(L_{left}, 6P)$ and $B(L_{right}, 6P)$

Bridges	x	y	z	$\dot{x}$	$\dot{y}$	$\dot{z}$	T	C
$B(L_{left}, 6P)$	0.54354320	0.95118448	0.20697067	0.14278533	−0.07925192	0.02312004	37.6272188	2.96837188
$B(L_{right}, 6P)$	0.55271068	0.96714914	−0.01749487	0.17535085	−0.09008381	0.17390770	37.6281296	2.96848535

are connected with a 11-bifurcation orbit in the 3D periodic family with stability index $-2\cos(2 \cdot 2\pi/11)$ in the curve p_1. Shown in the left figure of Fig. 9 are the T–C curves for the two *single-lane* bridges. The period of the 3D family is multiplied 11 times (in the figures, L' indicates the 2-bifurcation long period orbit on the left). To save space, we didn't give the curves p_1 and p_2 of these two bridges. For the 3-bifurcation long period orbits, the left one denoted as L' in Fig. 1 is the long period orbit with vertical stability index $2\cos(16 \cdot 2\pi/3)$, it is connected with a 16-bifurcation orbit in the 3D periodic family with stability index $-2\cos(3 \cdot 2\pi/16)$ in the curve p_1. The right one denoted as L in Fig. 10 is the long period orbit with vertical stability index $\cos(17 \cdot 2\pi/3)$, it is connected with a 17-bifurcation orbit in the 3D periodic family with stability index $-2\cos(3 \cdot 2\pi/17)$ in the curve p_1. Shown in the right figures of Fig. 9 are T–C curves for these two families. The period of the 3D periodic family is multiplied 16 times and 17 times respectively. The difference of these two bridges is that they are double-lane bridges. But since the two lanes of the bridge are two close, they are like one lane in the T–C curves.

For $\mu \in (\mu'_{k+1}, \mu'_k)$, if $p \geq 2$, the bridges $B(pL, qP)$ satisfy

$$p/(k+1)p < p/q < p/kp \tag{5}$$

For example, $p = 3$, there are bridges $(3L, (3k+2)P)$ and $B(3L, (3k+1)P)$; for $p = 5$, there are bridges $B(5L, (5k+4)P)$, $B(5L, (5k+3)P)$, $B(5L, (5k+2)P)$ and $B(5L, (5k+1)P)$. $q = k+1$ if $p = 1$.

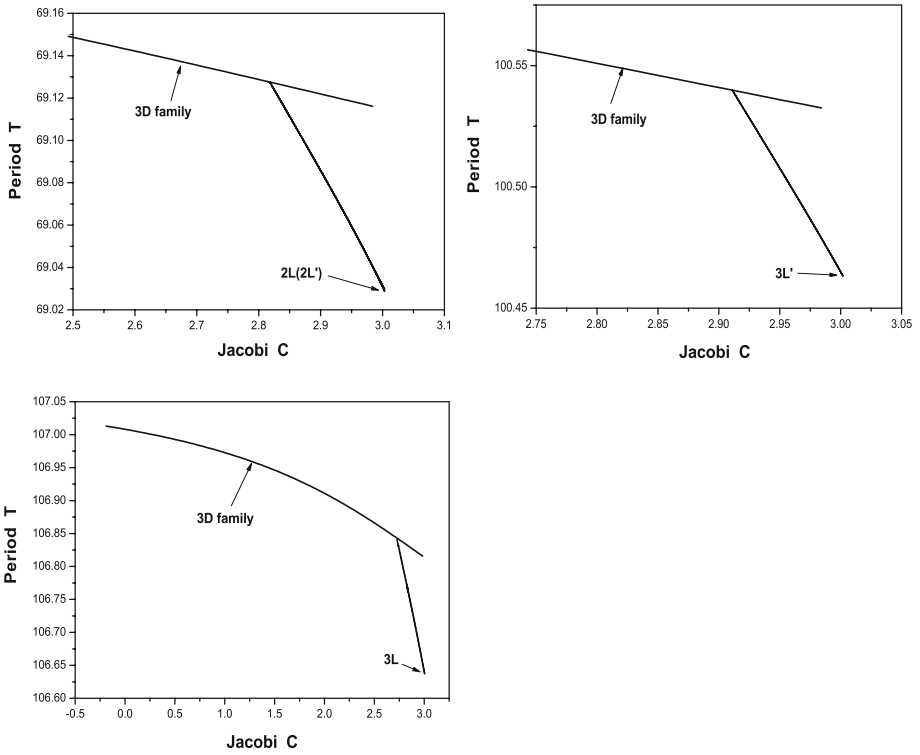

Fig. 9 The T–C curves for the single-lane bridge $B(2L, 11P)$, $B(2L', 11P)$ (top left figure) and the double-lane bridge $B(3L', 16P)$ (top right) and the double-lane bridge $B(3L', 17P)$ (bottom left)

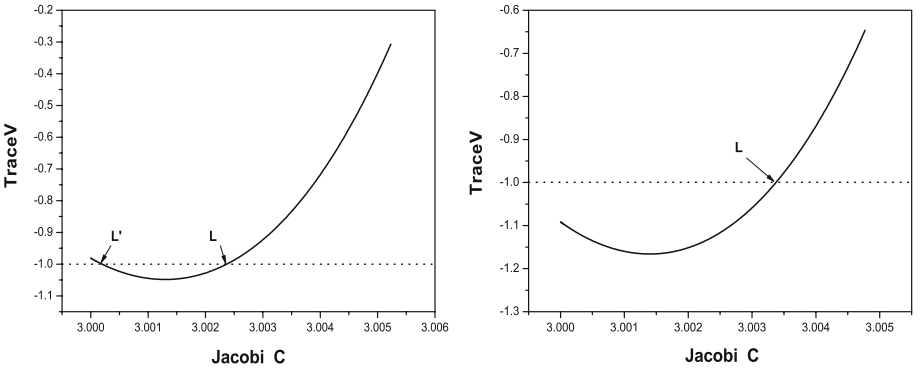

Fig. 10 The vertical stability curve of the long period family for $\mu'_{8/3} - 2 \times 10^{-5}$ and $\mu'_{8/3} + 1 \times 10^{-4}$

In fact, if $\mu_k > \mu > \mu'_{q/p} > \mu_{(2k+1)/2}$, there are always two p-bifurcation long periodic orbit (see the fourth figure in Fig. 3). We denote the one on the right of the stability curve as the orbit with stability parameter $2\cos(m \cdot 2\pi/p)$, $m < p/2$, and the one on the left as the orbit with stability parameter $2(\cos((p-m) \cdot 2\pi/p)$. Numerical explorations prove the following conclusion:

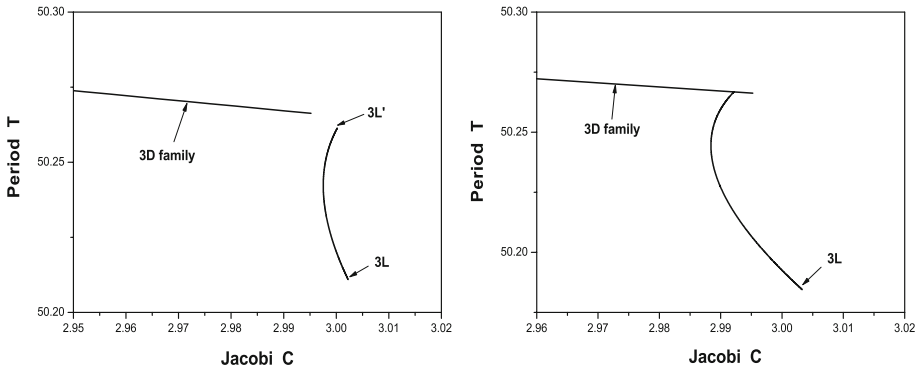

Fig. 11 The T–C curves of the bridge $B(3L, 3L')$ and $B(3L, 8P)$

(1) When p is an odd number, there are totally $p-1$ bridges $B(pL, qP)$ for fixed p. With $\mu < \mu_{[p(k+1)-i]/p}(1 \le i \le p-1)$, from the studies above, we know there are no p-vertical bifurcation long periodic orbit with stability index $2\cos(i \cdot 2\pi/p)$, and there is no $[p(k+1)-i]$-bifurcation 3D periodic orbit in the curve p_1 with stability index $2\cos(p \cdot 2\pi/[p(k+1)-i])$. So the bridge $B(pL, [p(k+1)-i]P)$ does not exist. With $\mu > \mu_{[p(k+1)-i]/p}$, the p-vertical bifurcation long periodic orbit and the $[p(k+1)-i]$-bifurcation 3D periodic orbit appear, so does the bridge $B(pL, [p(k+1)-i]P)$.

(2) When p is an even number, the evolution details are similar, but the number of bridges is different due to commensurability. For example, when $p=2$, there is the bridge $B(2L, (2k+1)P)$. When $p=4$, there should be three bridges $B(4L, (4k+3)P)$, $B(4L, (4k+2)P)$ and $B(4L, (4k+1)P)$. However, the bridge $B(4L, (4k+2)P)$ is in fact the bridge $B(2L, (2k+1)P)$, so there are only two bridges $B(pL, qP)$ for $p=2$. It's not hard to prove that when $p=2n$, there are only n bridges $B(pL, qP)$. The bridge $B(pL, (p(k+1)+1-2i)P)$, $1 \le i \le n$ connects the p-bifurcation long period orbit with the $(p(k+1)+1-2i)$-bifurcation 3D periodic orbit in the curve p_1.

Except $p=1$ or 2, all these bridges are double-lane bridges. Sometimes, the two lanes are too close to be separated by our numerical algorithms due to the limitation of accuracy, but they do be different lanes.

The existence of special critical values (Henrard 1970; Hou and Liu 2008a) may lead to the appearance of bridges $B(pL, pL')$, as in the planar case (Hou and Liu 2008b). Shown in Fig. 10 are the vertical stability curves for mass ratios $\mu'_{8/3} - 2 \times 10^{-5}$ and $\mu'_{8/3} + 1 \times 10^{-4}$. Due to the hollow in the stability curve, before μ increases to $\mu'_{8/3}$, two 3-bifurcation periodic orbits with stability index -1 appear. But the 8-bifurcation 3D periodic orbit doesn't appear yet. So the bridge $B(3L, 8P)$ doesn't exist. Instead, the two vertical bifurcation long period orbits are connected by the double-lane bridges $B(3L, 3L')$. When μ grows larger than $\mu'_{8/3}$, the orbit L' disappears and the 8-bifurcation 3D periodic orbit appears, the bridge $B(3L, 3L')$ disappears and the double-lane bridge $B(3L, 8P)$ appears. Shown in Fig. 11 are T–C curves for these two bridges.

The case of the vertical bifurcation families from the short period family is simpler. When $\mu < \mu_{q/p}$, there is no p-bifurcation short period orbit and q-bifurcation 3D periodic orbit in the curve p_2, so the bridge $B(pS, qP)$ does not exist. When $\mu < \mu_{q/p}$, the p-bifurcation short period orbit and q-bifurcation 3D periodic orbit in the curve p_2 appear, so does the

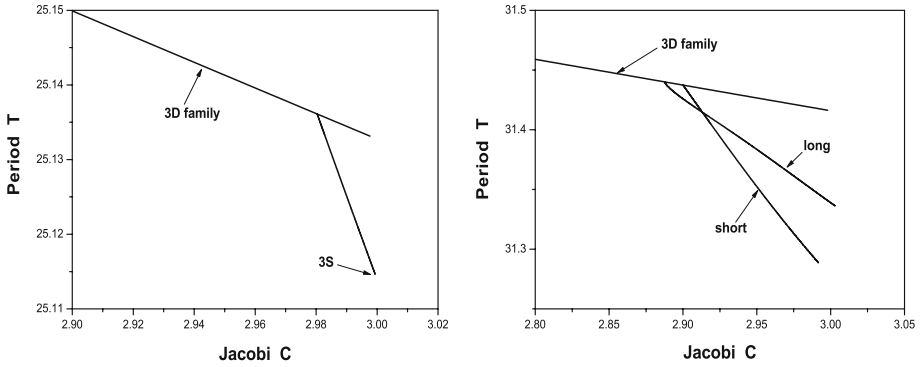

Fig. 12 The T–C curves of the bridge $B(3S, 4P)$ (left figure) and the bridges $B(4S, 5P)$ and $B(3L, 5P)$, for the same $q = 5$

bridge $B(pS, qP)$. Shown in the left figure of Fig. 12 are the stability curves of the family $B(3S, 4P)$. Remember, for the short period family, $1 < q/p < \sqrt{2}$.

From the discussions above, we know the following facts: The p-vertical bifurcation long period orbit is connected with a q-bifurcation orbit in the stability curve p_1 of the 3D periodic family by the bridge $B(pL, qP)$. The p-vertical bifurcation short period orbit is connected with a q-bifurcation orbit in the stability curve p_2 of the 3D periodic family by the bridge $B(pS, qP)$. Even for the same q, the bridges $B(pL, qP)$ and $B(pS, qP)$ are different, as shown in the right figure of Fig. 12. Except $p = 1$ or 2, all these bridges are double-lane bridges.

4 Conclusion

In this paper, following the increase of μ, we studied the evolution details of the vertical stability curves of the long and short period families and the 3D periodic family. We gave out the construction rules of the bridges $B(pL, qP)$ and $B(pS, qP)$ which connect vertical bifurcation long period and short period orbits with bifurcation orbits in the 3D periodic families. We also pointed out the existence of bridges of the kind $B(pL, pL')$ for some specific mass ratios.

Acknowledgement This work is supported by the National Natural Science Foundation of China (NSFC10673006, 10573040).

References

Bray, T.A., Goudas, C.L.: Three dimensional oscillations about L1, L2, L3. Adv. Astron. Astrophys. **5**, 71–130 (1967)

Bruno, A.D., Varin, V.P.: On families of periodic solutions of the restricted three-body problem. Celest. Mech. Dyn. Astr. **95**, 27–54 (2006)

Bruno, A.D., Varin, V.P.: Periodic solutions of the restricted three-body problems for small mass ratio. J. App. Math. Mech. **71**(6), 933–960 (2007)

Deprit, A., Henrard, J.: Natural families of periodic orbits. Astron. J. **72**(2), 158–172 (1967)

Deprit A., Henrard J.: A manifold of periodic orbits. In: Kopal Z. (ed.) Advances in Astronomy and Astrophysics, vol. 6, pp. 1–124. Academic Press (1968)

Hénon, M.: Vertical stability of periodic orbits in the restricted problem. Celest. Mech. **8**, 269–272 (1973)
Henrard, J.: Concerning the genealogy of long period families at L4. Astron. Astrophys. **5**, 45–52 (1970)
Henrard, J.: The web of periodic orbits at L4. Celest. Mech. Dyn. Astr. **83**, 291–302 (2002)
Hou, X.Y., Liu, L.: Another critical value concerning the genealogy of long period families at L4. Chin. J. Astron. Astrophys. **8**(1), 103–107 (2008a)
Hou, X.Y., Liu, L.: Bridges of the $B(pL, pL')$ kind around the triangular libration points. Astrophy. J. **678**, 1511–1516 (2008b)
Perdios, E., Zagouras, C.G.: Vertical stability of periodic solutions around the triangular equilibrium points. Celest. Mech. Dyn. Astr. **51**, 75–81 (1991)
Szebehely, V.: Theory of Orbits. Academic Press, New York (1967)
Zagouras, C.G.: Three-dimensional periodic orbits about the triangular equilibrium points of the restricted problem of three bodies. Celest. Mech. **37**, 27–46 (1985)